TECHNICAL ARTICLE

Mechanism and Control of Water Inrush from Separated Roof Layers in the Jurassic Coalfields

Yadong Ji[1,2] · Haidong Cao[1,2] · Baofeng Zhao[1,2]

Abstract

Theoretical analysis, numerical simulation, and borehole drilling were used to study the mechanism of four large-scale water inrush events that occurred during the mining of the 1121 working face in the Hongliu coal mine in the Ningdong mine area. We concluded that the working face inrush was induced by water in the bed separations formed by overlying strata movement caused by the mining process. To control such inrushes, the location, size, and hydrogeological properties of the 18 m thick key aquiclude were investigated. We determined that the best time to drain the bed separation water was between when the beds separated and the roof caved, before water inrush occurred. The best place to drain water from was directly above the key aquiclude. These results should be useful for other sites with similar mine conditions.

Keywords Separation space · Key aquiclude · Water inrush prevention technology

Introduction

A sandstone aquifer in the lower member of the Zhiluo Formation covers the primary mineable seam within the Jurassic Ningdong coalfield in western China and threatens the safe mining of the shallow coal seam, despite the fact it is a relatively weak aquifer (Ma et al. 2020; Zhao 2011). Large-scale and periodic water inrush events are relatively rare in mines with overlying weak sandstone aquifers as the direct water source (Jiang et al. 2015; Xu et al. 2011).

The mechanisms of roof water disasters have been previously researched. Ma et al. (2019) used numerical simulation and similar material simulation methods to investigate the coupled fault-separation, water-breaking mechanism under complex conditions in the Laohutai coal mine. Qiao et al. (2011) analyzed the basic conditions of the formation of separated layer water bodies, and revealed how hydrostatic water in separated layers above the stope roof could cause a "hydrostatic water inrush". Cui et al. (2020) studied the formation mechanism of a similar water disaster in the Xinjing

coal mine in Datong city, Shanxi Province. Fan et al. (2019) studied how to predict a stratified water inrush in coal mining in the Shle Wusu mining area, while Yin et al. (2019) studied the inrush mechanism of the quaternary aquifer in the roof of the Xinhe coal mine in Shandong. However, these few research studies on separation water inrushes are insufficient, and research on the mechanism of roof separation water disasters in the Jurassic coalfield is very rare.

There are many practical studies on overlying rock failures caused by coal mining (Banerjee et al. 2007; Cao 2017; Heather et al. 2017; Singh et al. 2007; Unver and Yasitli 2005; Wang et al. 2009).The key strata method is widely used to study overburden failures during mining, and predict water-conducted fissure height in coal seam roof strata (Chen and Zhu 2020; Liu et al. 2006; Ma et al. 2008; Majdi et al. 2012; Xu et al. 2012). However, no scholars have used this method to judge separation space and the location of separation water.

The rock failure process analysis software, RFPA^{2D}, is widely used in many disciplines to characterize overburden failure and simulate tunnel and rock failure processes (Kong et al. 2020; Liu et al. 2020; Wang and Yu 2010; Yang et al. 2020; Zhang 2009). Kong et al. (2020) developed RFPA^{2D} to simulate the separate failure processes of tunnels for different section types and different excavation methods. Liu et al. (2020) used RFPA^{2D} to investigate stress transfer under the various factors that influence mesoscopic fracturing of the

✉ Baofeng Zhao
sunman1220@163.com

1   Xi'an Research Institute, China Coal Technology and Engineering Group Corp., Xi'an 710077, China

2   Shaanxi Key Laboratory of Preventing and Controlling Coal Mine Water Hazard, Xi'an 710077, China

coal rock mass. Yang et al. (2020) used RFPA^{2D} to identify the borehole deformation region and stress changes after drilling in soft coal seams. In this study, we used theoretical analysis of key strata, RFPA^{2D} numerical simulation, and borehole drilling to investigate a working face water disaster induced by water in bed separations formed from overlying strata movement after coal mining.

Overview

The Study Area

The Ningdong coalfield is one of 14 large-scale coal production bases approved for construction in China and falls under the jurisdiction of the Ningxia Autonomous Region. The Hongliu coal mine is located in the southern Yuanyanghu mining area of the Ningdong coalfield (Fig. 1). The north–south strike length of the mine field is approximately 15 km, the east–west trend width is approximately 5.5 km, and the area covers approximately 79.55 km^2. The whole coalfield is divided into three horizontal zones and eight subzones, and the first level is divided into 12 mining zones that mine the #2, #3, and #4 coal seams. The second level is divided into 15 mining zones that mine coal seams #6, #10, and #12. The third level is divided into eight mining zones that mine the #15, #16, #17, and #18 coal seams.

Overview of the 1121 Working Face Water Disasters

The 1121 working face of the Hongliu coal mine was the first working face of the coalfield, targeting the #2 coal seam of the Jurassic Yan'an Formation. From November 2009 to March 2010, a total length of 186 m was mined, but four roof water disasters of different scales occurred. The maximum water inrush volume was 3000 m^3/h, which flooded the 1121 working face (Fig. 2). The direct water source was
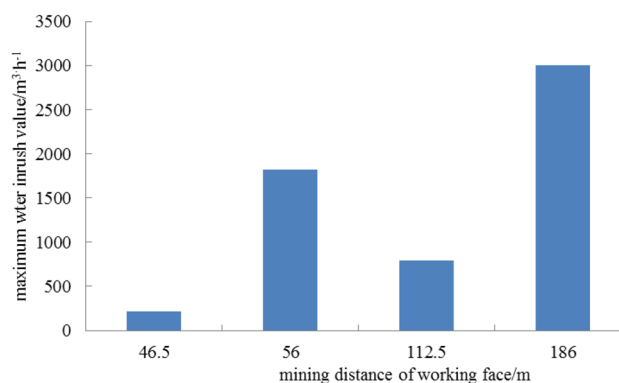

Fig. 2 The water inrush and its position in 1121 working face

the coarse sandstone aquifer of the lower section of the Zhiluo Formation, with a unit water inflow ranging from 0.010 to 0.094 L/(s·m). This is a weak aquifer, but large-scale roof water disasters still occur periodically. It was presumed that these inrushes were caused by water that accumulated in the void space created by roof strata separation.

Hydrogeological Conditions of the 1121 Working Face

According to drilling data, the direct roof of the #2 coal seam consists of 8–10 m of siltstone and fine sandstone (the no. 1 rock in Table 1). The roof base comprises the stratified coarse sandstone aquifer of the lower section of the Zhiluo Formation, with a thickness ranging from 14.66 to 47.17 m and an average thickness of 22.2 m (the no. 2 rock in Table 1). The upper part is a 7.0–25.5 m siltstone and mudstone aquiclude with an average thickness of 20 m (the no. 3 rock in Table 1) that expands and erodes when exposed to water. The upper stratified coarse sandstone aquifer of the lower section of the Zhiluo Formation ranges from 29.07 to 41.76 m in thickness, with an average thickness of 40.6 m;
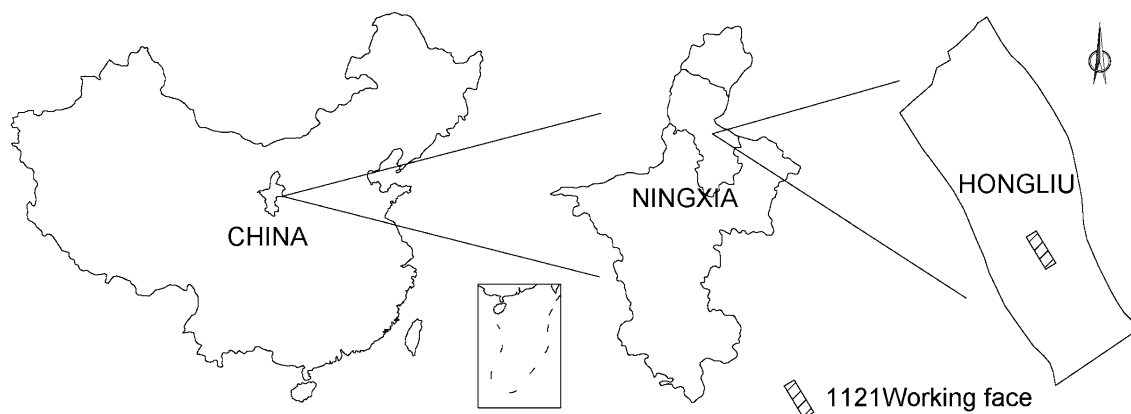

Fig. 1 The location of the study area

Table 1 Main physical parameters of the strata overlying the #2 coal seam

No	Geologic age	Aquifer (aquiclude)	Lithology	Thickness (m)	Saturated unit weight (kg m^{-3})	Compressive strength (MPa)	Strength of extension (MPa)	Cohesion (MPa)	Internal friction angle (°)	Elasticity modulus (10^4 MPa)	Poisson's ratio
10	Q	Aquifer	Surface soil	4	1.60	–	–	–	–	–	–
9	E	Aquiclude	Clay	45	2.00	–	–	–	–	–	–
8	J$_2$z	Aquiclude	Mudstone	76	2.46	15.2	0.82	1.92	35	0.8	0.20
7		Aquiclude	Fine sandstone	32	2.30	23.9	1.94	3.51	34	1.33	0.17
6		Aquiclude	Siltstone	14	2.31	23.5	1.29	3.18	34	1.05	0.16
5		Aquiclude	Fine sandstone	12	2.30	23.9	1.94	3.51	34	1.33	0.17
4		Aquifer	Coarse sandstone	40	2.18	19.8	1.38	3.07	34	1.43	0.17
3		Aquiclude	Mudstone	20	2.46	15.2	0.82	1.92	35	0.8	0.20
2		Aquifer	Coarse sandstone	22	2.18	19.8	1.38	3.07	34	1.43	0.17
1	J$_2$	Aquiclude	Siltstone	10	2.31	23.5	1.29	3.18	34	1.05	0.16
11			2#coal seam	5	1.45	–	–	–	–	–	–
12		Aquiclude	Siltstone	20	2.66	23.5	1.29	3.18	34	1.05	0.16

its lithology mainly consists of medium- and fine-grained sandstone and siltstone and a small amount of coarse-grained sandstone and mudstone. The cementation degree is low, revealing a highly unconsolidated structure, which easily breaks under hammer impact, disintegrates in water, and is very fragile. The mechanical parameters of each rock layer above the coal seam are listed in Table 1.

Locating the Water in the Separated Roof Strata

Determining the Separation Space

According to the key strata methodology, the lowest layer of the hard and thick strata of the overburden greatly influences the generation of the maximum separation layer. Considering that the other hard and thick strata of the overburden form a combined key layer, a separation layer occurs when the deflection of the strata does not immediately follow that of the main key layer. The fracturing of the rock layer above the main key layer often lags behind and a separation space is generated by the discontinuous movement between the various rock layers. Using the key stratum approach, Eq. (1) is used for the calculation.

$$E_{n+1}h_{n+1}^2 \sum_{i=1}^{n} \rho_i h_i > \rho_{n+1} \sum_{i=1}^{n} E_i h_i^3 \tag{1}$$

where E_n is the elastic modulus of each layer, n is the number of rocks in this group (arranged from bottom to top), h_n is the thickness of each layer, and ρ_n is the density of each layer. The positions of layers 2 and 1 are calculated as: $E_{n+1}h_{n+1}^2 \sum_{i=1}^{n} \rho_i h_i = 1.43 \times 22^2 \times 2.31 \times 10 = 15987.97$, and $\rho_{n+1} \sum_{i=1}^{n} E_i h_i^3 = 2.18 \times 1.05 \times 10^3 = 2289$.

The result of the first equation exceeds the result of second, which indicates that a separation space may develop over time between the two layers during the mining process. Since the first layer collapses with the mining of the working face, this separation space has no practical significance. The results indicate that separation space should evolve between layers 1 and 2, 3 and 4, 6 and 7, and 7 and 8.

Determining the Location of the Separation Water

The caving zone height of the 1121 working face of the Hongliu coal mine was 42.7 m, and the caving to mining ratio was eight based on borehole flushing fluid loss observations and borehole cameras. The height of the water-conducting fracture zone was 62.5 m and the ratio between the fracture and mining zones was 11.8. Mining of the 1121 working face has affected the bottom section of the Zhi-luo Formation coarse sandstone aquifer, i.e. layer no. 4.

Therefore, the separation spaces between layers 3 and 4, 6 and 7, and 7 and 8 could possibly be filled with water.

The main parameters controlling separation formation include the length l, the height h' of the separation layer along the mining direction of the working face, the distance H between the separation layer and coal seam, the distance S from the cut of the working face and the mining distance S_m from the working face. The migration characteristics of the overlying strata become increasingly trapezoidal with increasing stratum thickness, and the length of the established separation fissure also decreases, as shown in Fig. 3.

The calculation equation is given below:

$$l = h\sqrt{\frac{2\sigma_t}{q}} \tag{2}$$

where h is the caving rock mass thickness, σ_t is the tensile strength of the rock mass, and q is the sum of the loads of the rock mass itself and the overlying rock strata.

$$h' = M\eta - \frac{5q}{384EI}l^4 \tag{3}$$

where M is the mining thickness of the coal seam, η is the subsidence coefficient, q is the sum of the loads of the rock mass itself and the overlying rock strata, E is the elastic modulus of the rock mass, I is the moment of inertia of the rock mass, and L is the limit span of the rock mass, which is determined by Eq. (1).

$$H = \frac{M - h'}{K_p - 1} \tag{4}$$

where h' is the separation height and K_p is the breaking expansion coefficient.

$$S = H\cot\theta_2 + l/2 \tag{5}$$

$$S = H\cot\theta_1 + H\cot\theta_2 + l \tag{6}$$

where H is the distance from the separation space to the coal seam, L is the length of the separation layer along the working face mining direction, θ_1 is the fracture angle of the

rock layer on the cut side of the goaf, and θ_2 is the fracture angle of the rock layer on the side of the final mining line in the goaf.

As shown in Fig. 3, layer 3 is an elastic rock beam, and layer 4 is a rigid rock beam. The length of the separation layer along the mining direction of the working face is calculated according to Eq. (2).

$$l = \sqrt{\frac{2\sigma_t}{q}} = 78 \text{ m} \tag{2}$$

The separation height is calculated according to Eq. (3), with $h' = 2.296$ m; the relationship between the subsidence coefficient and the mining depth and thickness was obtained based on multiple observation stations. In combination with the lithologic conditions of the overlying strata of the Hongliu coal mine, the subsidence coefficient is 0.55. The distance between the separation layer and working face was calculated according to Eq. (4), at $H = 52.0$ m.

According to the research data, the average value of the fracture angle θ_1 on the cut side was 60°, and the average value of the fracture angle θ_2 on the side of the final mining line was 55°. The distance between the center of the separation layer and the working face was calculated with Eq. (5), at $S_m = 144$ m. Thus, given a key aquiclude that is 20 m thick, when 144 m of the working face is mined, a separation water storage space with a width of 78 m and a height of 2.3 m should have formed.

After the first occurrence of a separation space, the maximum separation space cyclically changes over time, but the distance between the separation space and the coal seam remains the same. Because the rock breaking angle on both sides of the goaf generates the first separation space when the working face mining length is calculated by Eq. (6), after the second separation space, the roof cyclically breaks, and the space delamination phenomenon periodically occurs during working face mining.

Because layer no. 4 is the main aquifer, it forms a separation water body, so only the section between layers 3 and 4 poses a threat to mining. Within the scope of the water-conducting fracture zone, the 20 m thick mudstone aquitard

Fig. 3 Schematic of the main control parameters (modified from Cao HD (2017))
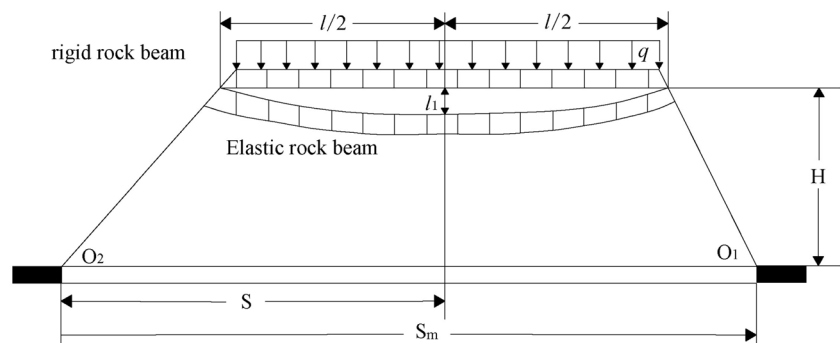
expands and disintegrates after being exposed to water, creating an initial water-filled space until the water-guiding fracture gradually fills with mudstone particles; when this occurs, the water-resistance of the layer redevelops and a separation water body is formed. The mudstone and its thickness are the key factors controlling the formation of reservoir separation between layers 3 and 4.

Numerical Simulation Analysis

Determination of the Simulation Experiment Scheme

Through a computer numerical simulation experiment with RFPA^{2D} software, assuming a constant mining thickness and overburden structure, the following was determined:

a. In the direction of the working face trend and tendency, the key aquiclude was increased from 7 to 22 m. For each increase of 1 m, a model was established to simulate the form, scope, and extent of the overlying stratum movement failure caused by mining.

b. The movement failure forms of the key control layer in the overburden rock were studied and the critical size of the key control layer was determined.

The whole model is composed of 12 layers including the coal strata, among which the fourth layer above the no. 2 coal seam is the main aquifer, and the third mudstone layer is the aquiclude. The model has a strike length of 600 m and a height of 300 m and is divided into 250×263 and 65,750 units, with horizontal constraints at both ends and a fixed bottom. For better caving, transverse joints were added between each layer. Excavation starts at 100 m to the left along the strike at a mining distance of 400 m. The stop-mining line was set at 100 m from the right boundary with 40 steps. The numerical calculation model is shown in Fig. 4.

Analysis of the Separation Formation Process

When the working face was mined to 30 m, the overlying strata were suspended, causing the bending rock beam to crack under the action of gravity, and the siltstone layer in the direct roof of the coal seam to separate, accompanied by the collapse of the first sandstone layer. When the working face mining depth reaches 60 m, a second large-scale collapse occurs, and the separation phenomenon develops rapidly upward. When the mining depth reaches 150 m, the separation space between the third and fourth layers reaches its maximum value, at which time the separation length is ≈76.8 m and the height is ≈2.5 m. Moreover, the height of the caving zone has reached the bottom of the third layer, namely, the aquiclude. When the working face mining depth
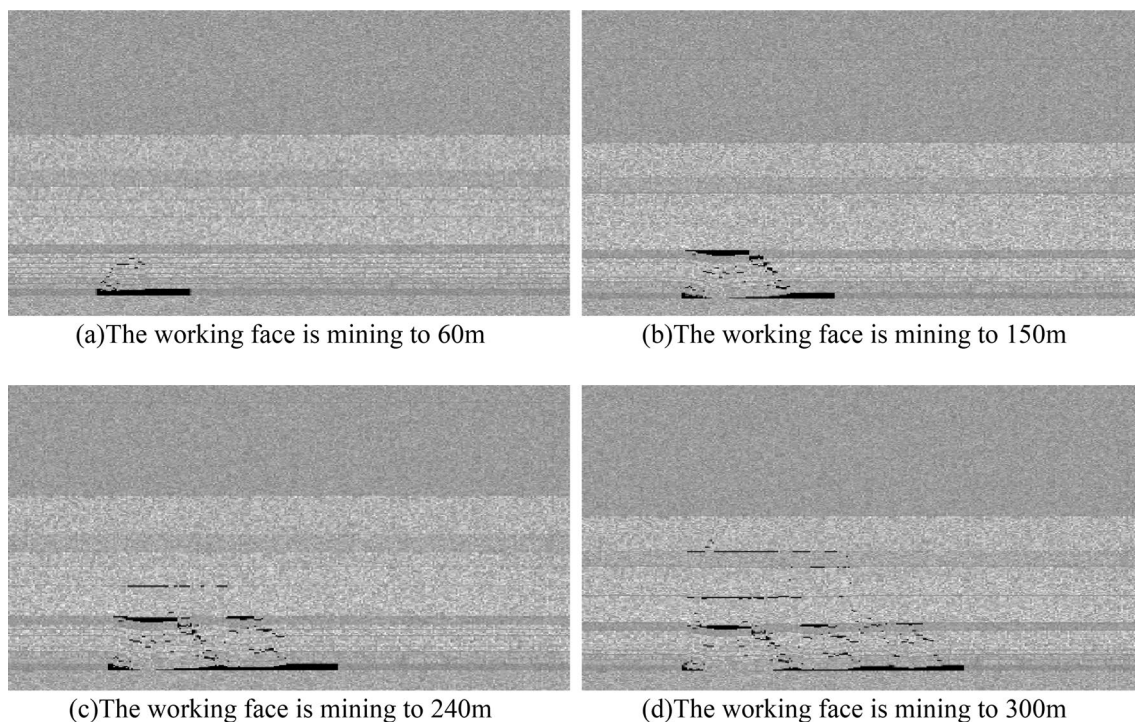
(a) The working face is mining to 60m

(b) The working face is mining to 150m

(c) The working face is mining to 240m

(d) The working face is mining to 300m

Fig. 4 Development process of the separation space (modified from Cao HD (2017))

reaches 240 m, the second separation space is ≈33.3 m in length and 1.3 m in height. A separation space ≈140 m in length and 0.3 m in height develops along the contact surface between the fifth and fourth layers. The height of the water-conducting fracture zone reaches the middle of the fourth layer, but the water-conducting fracture zone is filled with mudstone particles, and the groundwater in the aquifer does not flow into the working face.

When the working face mining depth reaches 300 m, a third separation space develops, but the second separation space does not increase. The first separation space gradually decreases due to compaction, with a notable decrease in length and height. The length of the separation space between the sixth and fifth layers is ≈152 m. When working face mining depth reaches 400 m (the final line), four stratifications occur between the third and fourth layers in the direction of working face mining. In addition, the length of the fourth separation space is ≈9.3 m, and the maximum height is ≈0.8 m. The separation spaces formed in the third, second, and first stages are gradually compacted, and the length and height are both greatly reduced. Moreover, a separation space develops along the contact surface and interior of the overburden from the second layer to the eighth layer, which is gradually compacted thereafter. In summary, fractures occur periodically in the third and fourth layers. The maximum height of the separation space is approximately 2.5 m, the maximum length of the separation space along the direction of the working face reaches approximately 76.8 m, and the distance between the separation spaces gradually decreases through compaction with the continued mining of the working face. The results are basically consistent with the theoretical analysis results.

Determining the Thickness of the Key Aquiclude

As stated above, the key mudstone aquiclude above the fully mechanized 1121 working face of the Hongliu coal mine is a significant factor determining whether a separation water

body is formed and whether the groundwater of the Zhiluo Formation aquifer enters the goaf.

Comparative Analysis of the Overburden Fracture

Due to space limitations, only the overburden fracture analysis for 18 and 21 m thick mudstone aquicludes is given here. When the mudstone aquiclude is 18 m thick, a separation space develops between the third and fourth layers when the working face mining length reaches 35 m. When the mining length is extended to 160 m, the maximum width of the separation space increases to ≈120 m, the maximum height reaches ≈1.1 m, and then it begins to close (Fig. 5a). Moreover, the fractures in the overburden penetrate the separation space and the separation water body extends into the goaf. Thus, the simulation indicates that water storage space does not periodically develop in the overburden. Therefore, when the thickness of the aquiclude is <18 m, the water-conducting fracture zone extends across the aquiclude and enters the bottom of the aquifer, and no obvious water body is formed (Fig. 5b).

When the mudstone aquiclude thickness is 21 m and the working face mining length reaches 40 m, a separation space developed between the third and fourth layers. With continuous mining of the working face, the water storage space gradually expands. When the working face is mined to 190 m, the maximum width of the water storage space increases to ≈81 m, the maximum height reaches ≈2.5 m, and closure then occurs (Fig. 6a). In addition, the fractures in the overburden still do not reach the separation space. Therefore, a water storage space occurs periodically, and the water-conducting fracture zone develops continuously upward until it increases to 58 m. After the mining simulation is completed, a periodic separation space occurs, with a period of ≈62 m. By the end of mining, the formation regularity of the separation water body is obvious (Fig. 6b).

When the aquiclude thickness is 19 m, the simulation results show that an 18 m thick water storage space is
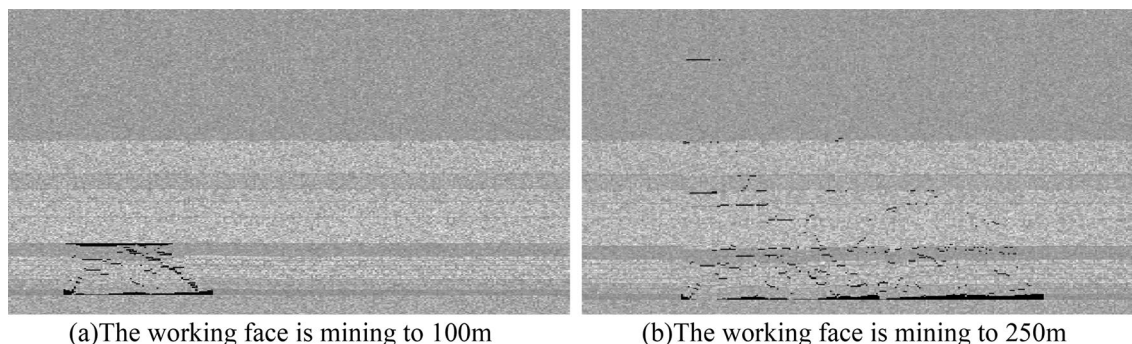

(a)The working face is mining to 100m   (b)The working face is mining to 250m

Fig. 5 The elastic modulus figure (the thickness of aquifuge is 18 m)

(a)The working face is mining to 100m

(b)The working face is mining to 100m
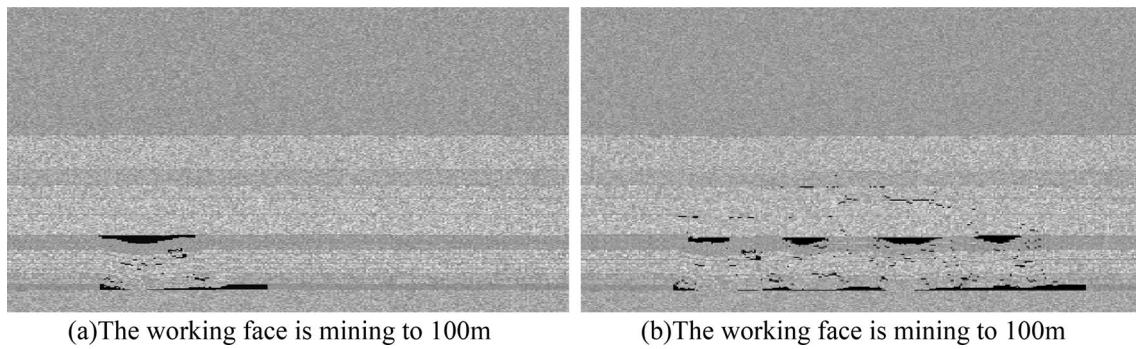
Fig. 6 Elastic modulus diagram (the thickness of the aquifuge is 21 m)

Comparative analysis of the seepage process

Vertical seepage velocity data at the bottom of the third key aquiclude and at the top of the mining coal seam were extracted from the RFPA numerical model. The seepage situation when the working face was mined to 300 m under the different aquiclude thicknesses is shown in Fig. 7.

For an aquiclude thickness of 10 m (Fig. 7a), the seepage velocity of the mudstone floor is much greater than that of

developed, and its regularity is greatly improved. Thus, the key aquiclude thickness is 18 m.

other areas within the range from the middle of the goaf to the cut side, and the maximum seepage velocity is ≈2.1 m/d. The distribution characteristics of the seepage velocity of the roof of the coal seam are the same as those of the mudstone floor. The goaf near the cut side attains the maximum seepage velocity, ≈2.4 m/d. Upper and lower conductive fractures have formed in the aquiclude, and the confined water in the main overlying aquifer enters the goaf through these conductive fractures, which ensures that the seepage velocities of the aquiclude and the coal seam roof are basically consistent. Under an aquiclude thickness of 14 m (Fig. 7b), the seepage velocity distribution areas of the mudstone floor,
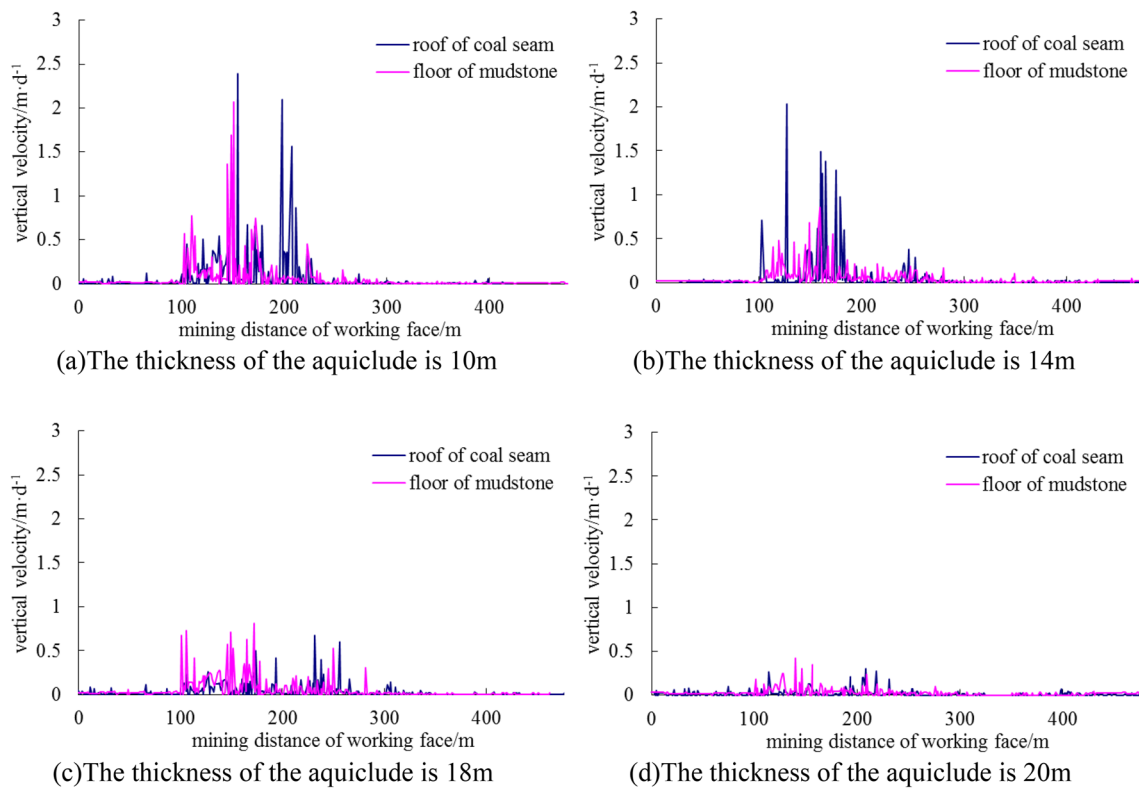

(a)The thickness of the aquiclude is 10m

(b)The thickness of the aquiclude is 14m

(c)The thickness of the aquiclude is 18m

(d)The thickness of the aquiclude is 20m

Fig. 7 Comparison of the seepage velocities under the different aquiclude thicknesses

(a) The duration curve of water drainage at the T2 drill site

(b) The duration curve of water drainage at the T4 drill site

(c) The duration curve of water drainage at the T5 drill site

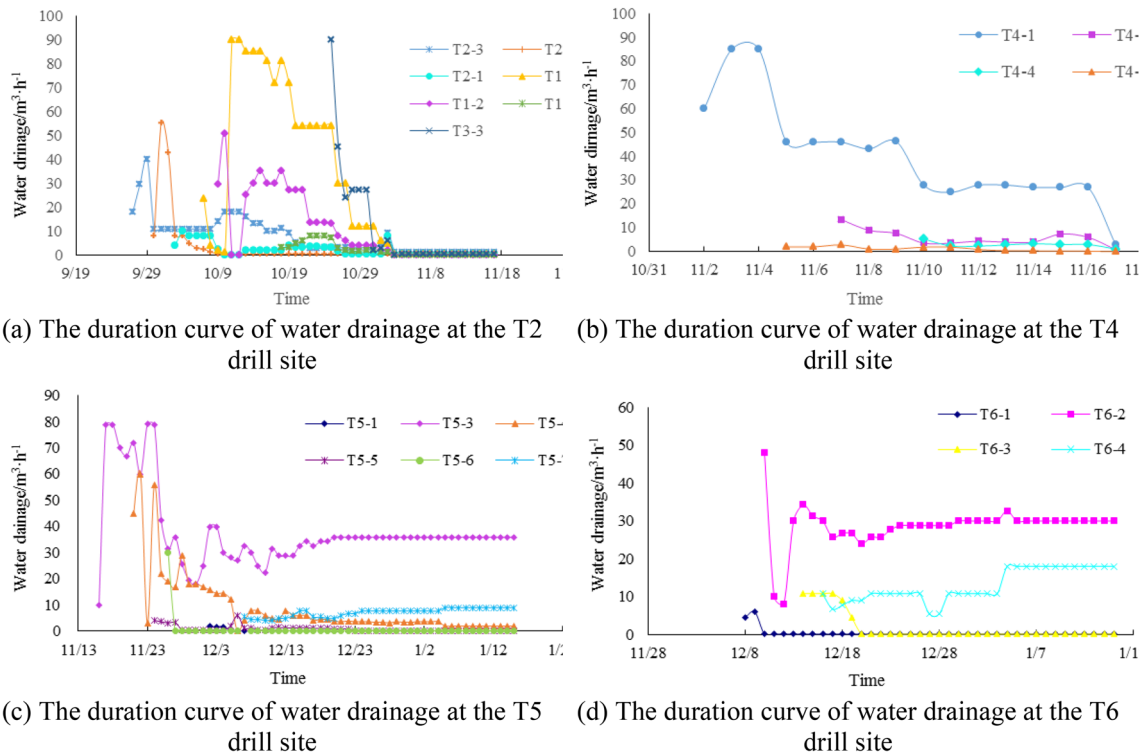(d) The duration curve of water drainage at the T6 drill site

Fig. 8 Duration curve of water drainage in each stage (modified from Cao HD (2017))

coal seam, and coal seam roof are still basically the same, among which the maximum seepage velocity of the mudstone roof is ≈1.1 m/d, and the maximum seepage velocity of the coal seam roof reaches ≈1.9 m/d.

For an aquiclude thickness of 18 m (Fig. 7c), the seepage velocity from the middle of the goaf to the cut side greatly decreases, and the maximum seepage velocity of the mudstone floor and coal seam roof is <0.8 m/d. For an aquiclude thickness of 20 m (Fig. 7d), the maximum seepage velocity of the mudstone floor and coal seam roof is <0.4 m/d.

In summary, when the aquiclude is more than 18 m thick, seepage through the mudstone floor and coal seam roof is greatly reduced. When the thickness of the aquiclude reaches 20 m, the seepage velocities are very low, indicating that the conductive fractures are nearly closed and that the water will not flow from the aquifer through the key aquiclude into the goaf.

Discussion

Analysis of Separation Water Disasters

With the continued mining of the working face, the direct roof of the coal seam collapses, and the aquiclude of the mudstone layer is deformed via subsidence, resulting in support loss. Due to the difference in tensile strength and

bending deflection between the mudstone aquicludes and sandstone aquifers, a separation space is formed between the sandstone and mudstone layers. When the thickness is larger than 18 m, the mudstone aquiclude expands under the action of the hydraulic effect, the mining-induced fractures gradually decrease, and a closed water storage space is then formed, after which water accumulates in the roof space. With increasing ceiling range, the aquiclude of the mudstone roof continues to creep and sink under the action of its own gravity and the mining and water pressures until it fails due to the resultant structural changes, and a separation water body prominently occurs. Multiple cycles lead to periodic water inrush. The regeneration process of the water isolation capacity plays a controlling role in the periodic water inrush phenomenon. This kind of permeable medium exhibits the characteristics of secondary hysteresis and periodicity.

Prevention and Control of Separation Water Disasters of the 1121 Working Face

Across the 240 m mining distance of the working face, the observed separation water drainage can be divided into six stages (at mining distances of 18, 45, 90, 120, 187, and 240 m). Figure 8 shows the water volumes during each drainage stage.

Through this sequential water drainage process, 240 m of the working face was safely mined from the stop-line of the

last water inrush accident. Twenty-five water drainage boreholes were designed and drilled in the machine and water drainage lanes, with a total drainage volume of ≈212,000 m³. During the mining of the working face, no obvious abnormal water inflow occurred, and the water inflow from the goaf basically remained stable at 130–150 m³/h.

Conclusion

A key aquiclude in the overburden is a necessary condition for substantial amounts of water to accumulate in the voids that form between separated overburden strata. The overburden failure process was analyzed, and a key aquiclude thickness of 18 m was proposed for this mine site. The processes of mudstone bending, sinking, creep, fracture, and closure were verified. The controlling effect of the key aquiclude on the periodic water inrush phenomenon was revealed. The optimal water drainage time and spatial position of the separation water bodies were determined.

References

Banerjee G, Kushwaha A, Kumbhakar D (2007) Prediction of strata and support behaviour during shortwall mining of developed bord & pillar workings at Balarampur Mine. SECL Indian Min Eng J 46(11):146–160

Cao HD (2017) Mechanism and control technology of water inrush from secondary separated bed on coal seam roof. Coal Geol Explor 45(6):90–95 (in Chinese)

Chen Y, Zhu SY (2020) Determination of caved and water-conducting fractured zones of "two soft and one hard" unstable coal seam. Acta Geod Geophys 55(3):451–475. https://doi.org/10.1007/s40328-020-00300-w

Cui FP, Wu LL, Wu Q, Xiong Ch, Jin C, Li N, Liu DM (2020) Formation mechanism of a disastrous groundwater inrush occurred at the Xinjing coal mine in Datong, Shanxi Province, China. Geomatics Nat Hazards Risk 11(1):559–571. https://doi.org/10.1080/19475705.2020.1736189

Fan KF, Li WP, Wang QQ, Liu SL, Xue S, Xie CY, Wang ZK (2019) Formation mechanism and prediction method of water inrush from separated layers within coal seam mining: a case study in the Shilawusu mining area, China. Eng Fail Anal 103:158–172. https://doi.org/10.1016/j.engfailanal.2019.04.057

Heather EL, Douglas T, Mark KL, Habte A (2017) Effects of overburden characteristics on dynamic failure in underground coal mining. Int J Min Sci Tech 27(1):121–129. https://doi.org/10.1016/j.ijmst.2016.10.001

Jiang JQ, Wang P, Wu QL, Zhang PP (2015) Evolution laws and prediction of separated stratum space under overlying high-position magmatic rocks. Chin J Geotech Eng 37(10):1769–1779 ((in Chinese))

Kong XY, Chen X, Tang CA, Sun ZR, Hu EH (2020) Study on large deformation control technology and engineering application of tunnel with high ground stress and weak broken surrounding rock. Struct Eng Int. https://doi.org/10.1080/10168664.2020.1770664

Liu WQ, Gu ZH, Wang B, Miao XX (2006) Coupling action of water-resisting roof layer and key strata. J China Univ Min Tech 35(4):427–430 ((in Chinese))

Liu JW, Liu CY, Li XH (2020) Stress transfer law and its influencing factors of mesoscopic fracturing of coal rock mass. Arab J Geosci 13:599. https://doi.org/10.1007/s12517-020-05544-y

Ma YJ, Wu Q, Zhang ZY, Hong YQ, Guo LW, Tian HSH, Zhang LG (2008) Research on prediction of water conducted fissure height in roof of coal mining seam. J China Coal Sci Tech 36(5):59–62 ((in Chinese))

Ma LJ, Zhao BF, Xu HJ, Cao HD (2019) Research on water inrush mechanism of fault coupling bed separation with fully-mechanized sublevel caving of ultra-thick coal seam. J China Coal Soc 44(2):567–575 ((in Chinese))

Ma LJ, Zhao BF, Wang H, Gao Y (2020) Analysis of spatial differences in permeability based on sedimentary and structural features of the sandstone aquifer overlying coal seams in western China. Mine Water Environ 39(2):229–241. https://doi.org/10.1007/s10230-020-00682-x

Majdi A, Hassani FP, Nasiri MY (2012) Prediction of the height of destressed zone above the mined panel roof in longwall coal mining. Int J Coal Geol 98:62–72. https://doi.org/10.1016/j.coal.2012.04.005

Qiao W, Li WP, Li XQ (2011) Mechanism and prevention of "hydro-static water inrush" of roof separation water in stope. J Min Safety Eng 28(1):96–104 ((in Chinese))

Singh R, Mandal PK, Singh AK, Kumar R, Matiti J, Ghosh AK(2007) Upshot of strata movement during underground mining of a thick coal seam below hilly terrain. Int J Rock Mech Min Sci 45(1). https://doi.org/10.1016/j.ijrmms.2007.03.006

Unver B, Yasitli NE (2005) Modelling of strata movement with a special reference to caving mechanism in thick seam coal mining. Int J Coal Geol 66(4). https://doi.org/10.1016/j.coal.2005.05.008

Wang JM, Yu DH (2010) Simulation of water hazards caused by burst of water cells formed by overburden stratum separation. Chin J Geotech Eng 32(2):231–236 ((in Chinese))

Wang Z, Zhou H, Xie H (2009) Research on fractal characterization of mined crack network evolution in overburden rock stratum under deep mining. Rock Soil Mech 30(8):2403–2408 ((in Chinese))

Xu LC, Guo YH, Huang XL, Liu L (2011) Simple analysis of main water bursting type and prevention and control technology in China coal mine. Safety Coal Mines 42(1):53–56 ((in Chinese))

Xu JL, Zhu WB, Wang XZ (2012) New method to predict the height of fractured water-conducting zone by location of key strata. J China Coal Soc 37(5):762–769. https://doi.org/10.1007/s11783-011-0280-z

Yang S, Wen GC, Yan FZ, Zhang MJ, Zhao XS (2020) Evaluating the maximum rate of penetration for drilling borehole in soft coal seam. Energy Sci Eng 8:3273–3284. https://doi.org/10.1002/ese3.724

Yin HY, Zhao H, Xie DL (2019) Mechanism of mine water inrush from overlying porous aquifer in quaternary: a case study in Xinhe coal mine of Shandong Province. China Arab J Geosci 12(5):163. https://doi.org/10.1007/s12517-019-4325-0

Zhang YJ (2009) Numerical simulation on forecasting water inflow and characteristic of overburden failure based on fluid-solid coupling theory. J China Coal Soc 34(5):610–613 ((in Chinese))

Zhao L (2011) Sedimentary characteristics and its hydrogeological significance of Jurassic Zhiluo Formation in the east of Ning Xia Province. MS Diss, College of Geological Science & Engineering, Shan Dong, China (in Chinese)